https://doi.org/10.5194/essd-2026-350
Preprint. Discussion started: 11 June 2026

Open Access Earth System Science Data Discussions

Caravan-CMIP6: Bias-corrected climate model projections for ten large-sample hydrometeorological datasets and over 23,000 global catchments

Sacha W. Ruzzante[1]

[1]University of Victoria, Victoria, V8P 5C2, Canada

Correspondence to: Sacha W. Ruzzante (sruzzante@uvic.ca)

Abstract. This data paper introduces Caravan-CMIP6, a dataset of climate change projections for large-sample hydrologic studies. Caravan-CMIP6 includes projections from an ensemble of 12 climate models from the sixth Coupled Model Intercomparison Project (CMIP6), for the historical experiment (1850-2014) and three Shared Socio-economic Pathways (SSPs). The dataset includes projections for all catchments within ten large-sample hydrometeorological datasets: Caravan, CAMELS, CAMELS-AUS-v2, CAMELS-BR, CAMELS-CH CAMELS-CL, CAMELS-COL, CAMELS-DE, CAMELS-GB-v2, CAMELS-IND. For each large-sample hydrometeorological dataset, I provide CMIP6 projections for all meteorological variables that can be readily extracted from climate models, including precipitation, temperature, evapotranspiration, humidity, radiation, pressure, and wind speed. I bias-correct the climate model output to match the observed climatology within each dataset. This dataset can facilitate the use of large-sample hydrologic datasets and models for climate change projection. All raw and bias-corrected data are available at https://doi.org/10.20383/103.01644.

Short Summary: Caravan-CMIP6 provides climate change projections of weather for many rivers worldwide. Using Caravan-CMIP6, researchers will be able to use existing hydrologic models, which are calibrated on historical data, to predict future river flows under three climate change scenarios.

1 Introduction

Large-sample hydrometeorological datasets (herein referred to as LSH datasets) have significantly advanced the field of hydrology in recent years. These datasets include streamflow, catchment characteristics, and meteorological data for typically hundreds or thousands of catchments. They have enabled highly skilled hydrologic predictions, hydrologic model intercomparison studies, investigations of modelling best-practices, and large-scale analyses of hydrologic processes (Arsenault et al., 2023; Berghuijs et al., 2025; Brunner et al., 2025; Feng et al., 2022; Kraft et al., 2025; Kratzert et al., 2019; Lees et al., 2021; Ruzzante et al., 2026; Shen et al., 2022).

Since the development of the first CAMELS dataset for the United States (Addor et al., 2017; Newman et al., 2015), others have extended the concept in various ways: (i) creating datasets for new locations (*e.g.* Alvarez-Garreton et al., 2018) (ii)

https://doi.org/10.5194/essd-2026-350
Preprint. Discussion started: 11 June 2026

including sub-daily streamflow and meteorology (*e.g,* Tran et al., 2025), (iii) including water quality data (*e.g,* do Nascimento et al., 2025), (iv) including spatially distributed meteorology (*e.g.,* Knoben et al., 2025), and (v) including short-range meteorological forecasts (Shalev and Kratzert, 2024). Since LSH datasets often focus on near-natural catchments with long time series of high-quality streamflow data, they have significant potential to be used for climate change studies. Some authors have used the CAMELS and HYSETS databases (Addor et al., 2017; Arsenault et al., 2020; Newman et al., 2015) to evaluate the suitability of models and approaches to simulate climate change impacts (Dallaire et al., 2021; Feng et al., 2023; Martel et al., 2025; Rahimpour Asenjan et al., 2023) and also to predict responses to climate change (Castaneda-Gonzalez et al., 2023b, a; Chen et al., 2023; Wu et al., 2022). However, climate model projections from the sixth Climate Model Intercomparison Project (CMIP6) have not been compiled and made available for most CAMELS-style datasets.

Here I present bias-corrected CMIP6 climate model projections for the Caravan dataset and nine CAMELS-style datasets. A full set of relevant hydrometeorological parameters from CMIP6 models are bias-corrected to match the hydrometeorological data in each LSH dataset, including precipitation, air temperature (mean, maximum, and minimum), potential and actual evapotranspiration (Penman-Monteith, Hargreaves, Priestly-Taylor, and Morton estimates), atmospheric pressure, shortwave and longwave radiation, wind speed, and humidity (relative humidity, dewpoint temperature, and vapour pressure).

This set of climate model projections can enable several avenues of inquiry. First, for individual users of these datasets it will significantly reduce the barrier-to-entry to project flows under climate change. Extracting climate model projections and bias-correcting them requires some technical knowledge that not all hydrologists possess, or need to possess. The computation required for this is also expensive, in terms of storage (tens of TB) and processing time (hundreds of CPU-equivalent years), which not all researchers have access to, and which generates substantial climate-warming emissions. Second, I anticipate that this dataset will enable model intercomparison studies to examine how different model structures translate into differences in projected future conditions.

2 Methods

2.1 Large-Sample Hydrology datasets

I produce bias-corrected CMIP6 ensembles for the Caravan dataset (including all extensions as of 15 November, 2025) (Kratzert et al., 2023), as well as CAMELS (Addor et al., 2017; Newman et al., 2015), CAMELS-AUS-v2 (Fowler et al., 2025), CAMELS-BR (Chagas et al., 2020), CAMELS-CH (Höge et al., 2023), CAMELS-CL (Alvarez-Garreton et al., 2018), CAMELS-COL (Jimenez et al., 2025), CAMELS-DE (Loritz et al., 2024), CAMELS-GB-v2 (Coxon et al., 2025), CAMELS-IND (Mangukiya et al., 2025). Table S1 lists these datasets along with the meteorological data included by each.

https://doi.org/10.5194/essd-2026-350
Preprint. Discussion started: 11 June 2026

It is only possible to bias-correct meteorological variables that are reported by CMIP6 models, or which can be derived from CMIP6 model data. This includes air temperature, precipitation, relative humidity, air pressure, wind speed, and radiation variables.

I therefore must exclude some variables included in some of the CAMELS datasets. These variables include soil moisture (eg. Kratzert et al., 2023; Mangukiya et al., 2025), actual evapotranspiration (eg. Höge et al., 2023; Mangukiya et al., 2025) except by the algorithm developed by Morton (1983), potential evapotranspiration with corrections for interception (eg. Coxon et al., 2025; Höge et al., 2023; Mangukiya et al., 2025), relative sun duration (Höge et al., 2023), and relative humidity at the time of maximum/minimum temperature (Fowler et al., 2025).

Snow-water equivalent is reported by some climate models, and is also included in Caravan (Kratzert et al., 2023). However, the ERA5-Land data from which Caravan is extracted represents glaciers as a snow-water equivalent of 10 m (Muñoz Sabater, 2019), and the classification of glacier cover contains some temporal discontinuities. This leads to discontinuities in the Caravan snow-water equivalent data for some glaciated catchments. These discontinuities cause instabilities in the bias correction algorithm, so I excluded this variable.

It is also not possible to provide spatial medians, minimums, maximums, or standard deviations (eg. Loritz et al., 2024) since the CMIP6 models are provided on very coarse-resolution grids (50 km to 500 km), such that some catchments fall entirely within one grid cell.

2.1 Ensemble Selection

The CMIP6 models included in this dataset are listed in Table 1. The models were chosen following Mahony et al. (2022), with some modifications made. I required each model and variant to report nine variables (variable abbreviations and definitions are provided in the appendix):

- Precipitation: pr
- Mean temperature: tas
- Maximum temperature: tasmax
- Minimum temperature: tasmin
- Relative humidity: hurs
- Pressure: ps OR psl
- Wind speed: (uas AND vas) OR sfcWind
- Shortwave radiation: (rsds AND rsus) OR rss
- Longwave radiation: (rlds AND rlus) OR rls

I also required each model and variant to report results for the historical experiment and at least two of the three scenarios (ssp126, ssp245, and ssp585).

With these constraints I made the following modifications to the ensemble selected by Mahony et al. (2022):

- GFDL-CM4 was substituted for GFDL-ESM4 because the latter is missing rsus and rlus variables.

https://doi.org/10.5194/essd-2026-350
Preprint. Discussion started: 11 June 2026

Open Access Earth System Science Data Discussions

- BCC-CSM2-MR was removed because it is missing hurs.
- CNRM-CM6-1-HR was substituted for CNRM-ESM2-1 because the latter was missing rsus.
- GISS-E2-1-G was removed because it is missing rsus, rlus, psl, ps, hurs, uas, and vas
- No models built on the widely-used and respected Community Earth System Model (CESM) (Hurrell et al., 2013) were included by Mahony et al. (2022) because at that time these models were missing tasmin and tasmax. I included TaiESM1, which is built on CESM and reports a full suite of variables.

Figure 1 shows the global average temperature rise above preindustrial conditions (1850-1899) for each model. CMIP6 includes a number of models that are 'too hot': they have Equilibrium Climate Sensitivities (ECS) and Transient Climate Responses (TCR) above the ranges that have been assessed from multiple lines of evidence (Hausfather et al., 2022; Sherwood et al., 2020). For ECS these ranges are 2ºC-5ºC (*very likely*) and of 2.5C-4ºC (*likely*). For TCR the ranges are 1.2C-2.4ºC (*very likely*) and 1.4C-2.2ºC (*likely*).

At least four approaches have been proposed to deal with the 'hot model problem':

1) Base projections on global warming levels rather than scenarios (Bevacqua et al., 2026; Hausfather et al., 2022; James et al., 2017). The full ensemble can then be used. In Table 1 below I provide 30-year periods for each model for which the average global warming above preindustrial levels is equal to 1.5ºC, 2ºC, 3ºC, and 4ºC. These year ranges are based on the ssp585 scenario. This is the recommended approach if the warming trajectory is not of concern (Hausfather et al., 2022).
2) Remove models whose ECS lies outside the *likely* range of 2.5C-4ºC range or outside the *very likely* range of 2ºC-5ºC (Hausfather et al., 2022; Mahony et al., 2022). In this ensemble five models fall within the *likely* range (**bold and underlined** in Table 1) and nine within the *very likely* range (**bold**).
3) Remove models whose transient climate response (TCR) lies outside the *likely* range of 1.4C-2.2ºC range or outside the *very likely* range of 1.2ºC-2.4ºC (Hausfather et al., 2022). In this ensemble the inclusion/exclusion criteria are identical to those derived from the ECS ranges except for CNRM-CM6-1-HR (within 'very likely' range of ECS, above 'very likely' range of TCR), and INM-CM5-0 (below 'very likely' range of ECS, within 'likely' range of TCR. The likely and very likely ranges are bolded and underlined in the same manner as the ECS values in Table 1.
4) Use all models but weight model projections to match the assessed distribution of ECS (Cannon, 2024b). Here I provide weights that satisfy this condition following the strategy proposed by Cannon, (2024b).

Table 1: Ensemble of 12 CMIP6 models included in Caravan-CMIP6, along with their equilibrium climate sensitivity (ECS) and transient climate response (TCR). N is the number of variants included. The following four columns indicate 30-year periods for which the global mean temperature rise first exceeds each temperature threshold. Weights are also provided if users wish to weight projections to match the assessed distribution of ECS (Cannon, 2024b).

Source ID	ECS	TCR	N	1.5ºC	2ºC	3ºC	4ºC	Weights	Citation
ACCESS-	**3.88**	**1.97**	10	2006-2035	2016-2045	2035-2064	2052-2081	0.14	(Ziehn et

https://doi.org/10.5194/essd-2026-350
Preprint. Discussion started: 11 June 2026

ESM1-5									al., 2020)
CNRM-CM6-1-HR	**4.34**	2.46	1	2004-2033	2016-2045	2036-2065	2052-2081	0.02	(Voldoire et al., 2019)
CanESM5	5.64	2.71	10	1993-2022	2003-2032	2022-2051	2037-2066	0.02	(Swart et al., 2019)
EC-Earth3	**4.26**	**2.3**	3	2006-2035	2021-2050	2040-2069	2055-2084	0.03	(Döscher et al., 2022)
GFDL-CM4	**3.89**	**2.00**	1	2015-2044	2026-2055	2046-2075	2064-2093	0.13	(Held et al., 2019)
INM-CM5-0	1.92	**1.41**	1	2017-2046	2032-2061	2060-2089	2097-2100	0.01	(Volodin and Gritsun, 2018)
IPSL-CM6A-LR	**4.70**	**2.35**	6	1993-2022	2005-2034	2023-2052	2038-2067	0.03	(Boucher et al., 2020)
MIROC6	**2.60**	**1.55**	3	2025-2054	2038-2067	2059-2088	2089-2100	0.25	(Tatebe et al., 2019)
MPI-ESM1-2-HR	**2.98**	**1.64**	1	2018-2047	2034-2063	2059-2088	2085-2100	0.19	(Mauritsen et al., 2019)
MRI-ESM2-0	**3.13**	**1.67**	5	2012-2041	2024-2053	2048-2077	2069-2098	0.14	(Yukimoto et al., 2019)
TaiESM1	**4.36**	**2.27**	1	2007-2036	2015-2044	2029-2058	2041-2070	0.02	(Lee et al., 2020)
UKESM1-0-LL	5.36	2.77	5	2006-2035	2016-2045	2032-2061	2046-2075	0.02	(Sellar et al., 2019)

125

https://doi.org/10.5194/essd-2026-350
Preprint. Discussion started: 11 June 2026

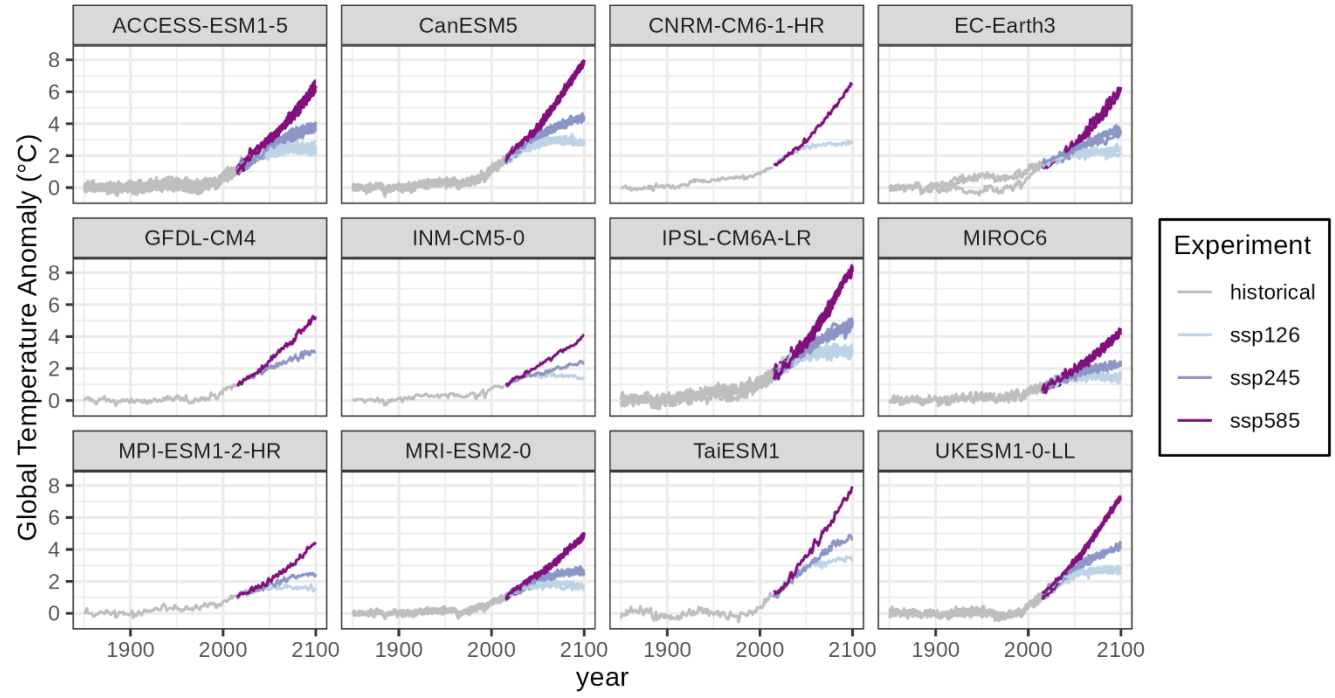

Figure 1: Global mean temperature rise predicted by each model in the ensemble, relative to preindustrial conditions (1850-1899). All variants from each model are plotted.

2.2 Raw CMIP6 model output extraction

I extract the raw data from each CMIP6 raster dataset using the basin polygons from each CAMELS dataset and the extract function in the R package terra (Hijmans et al., 2026). I take the average of all grid cells partially or full covered by each basin polygon weighted by the percentage overlap.

2.3 Bias Correction

For each LSH dataset I bias-correct climate model output to match meteorological observations from 1981-2010 using Quantile Delta Mapping (QDM) from the MBC R package (Cannon, 2024a; Cannon et al., 2015). Following Cannon et al. (2022) the bias correction is applied using sliding windows both within and across years. I use 30-year sliding windows from 1850 to 2014 (historical experiment) and 2015 to 2100 (ssp126, ssp245, and ssp585 scenarios), replacing the central 10 years within each 30-year window. To preserve the seasonality of the observed meteorological data, I divide the year into 24 'half-months'. I bias correct each half month separately, using a sliding window of three half months. The first half of each month is always defined as the first 15 days regardless of the length of the month or the calendar used by each climate model.

I bias-correct temperature, relative humidity, pressure, and dewpoint temperature as interval quantities (preserving absolute changes in the projections) and precipitation, wind speed, vapour pressure, potential evapotranspiration, and net solar

https://doi.org/10.5194/essd-2026-350
Preprint. Discussion started: 11 June 2026

radiation as ratio quantities (preserving relative changes). Net thermal (longwave) radiation can be negative or positive, so it was necessary to treat this as an interval quantity.

The bias-correction has the potential to introduce a small number of unrealistic or impossible values. I impose the following limits on the bias-corrected data:

Relative humidity is constrained between 0% and 100 %, vapour pressure is constrained to be less than the saturation vapour pressure at the daily mean temperature, and dewpoint temperature is constrained to be less than or equal to the daily mean temperature.

The daily minimum temperature must be less than or equal to the daily mean temperature, and the daily maximum temperature must greater than or equal to the daily mean temperature. For datasets with only minimum and maximum temperature, the minimum temperature must be less than or equal to the maximum temperature.

For solar radiation variables (rsds and rss) the values are limited to 1400 W m^{-2}, which is approximately the maximum possible extraterrestrial radiation at the top of the atmosphere (Allen et al., 1998).

Precipitation is limited to 3476.7 mm/day, which is the maximum value that can be stored as a signed 16-bit integer with the scaling settings used here. This is approximately 1.8 times larger than the world record 24-hour point precipitation recorded at Foc-Foc on 26 January 1966 (Cerveny et al., 2007).

2.3.1 Transformations of raw climate model outputs

The climate model output variables are not always provided in the same form as the variables provided in the observed meteorological data, or are not in the optimal form for bias correction. Several transformations of the raw climate model output are therefore applied prior to bias correction. These transformations are applied to the raw basin-averaged outputs.

Following Thrasher et al. (2012), to preserve physically realistic relationships between mean, maximum, and minimum daily air temperature (tas, tasmax, and tasmin), the mean temperature is first bias corrected and the differences are then bias corrected:

$$\mathrm{tasmax}_{\mathrm{diff}} = \mathrm{tasmax} - \mathrm{tas} \quad (1)$$

$$\mathrm{tasmin}_{\mathrm{diff}} = \mathrm{tasmin} - \mathrm{tas} \quad (2)$$

The bias-corrected maximum and minimum temperatures are then recalculated:

$$\widehat{\mathrm{tasmax}} = \widehat{\mathrm{tas}} + \widehat{\mathrm{tasmax}}_{\mathrm{diff}} \quad (3)$$

$$\widehat{\mathrm{tasmin}} = \widehat{\mathrm{tas}} + \widehat{\mathrm{tasmin}}_{\mathrm{diff}} \quad (4)$$

Where the hat accent denotes a bias-corrected value.

For datasets that only provide tasmin and tasmax, tasmax and the diurnal range are bias corrected and tasmin is calculated by subtracting the diurnal range from the maximum temperature.

Within the climate models net surface shortwave (rss) and longwave radiation (rls) and not always provided, so they are calculated as the difference between downwelling (rsds and rlds) and upwelling (rsus and rlus) components:

https://doi.org/10.5194/essd-2026-350
Preprint. Discussion started: 11 June 2026

Open Access Earth System Science Data Discussions

$$\mathrm{rss} = \mathrm{rsds} - \mathrm{rsus} \tag{5}$$

$$\mathrm{rls} = \mathrm{rlds} - \mathrm{rlus} \tag{6}$$

Shortwave and longwave radiation are considered equivalent to solar and thermal radiation, respectively.

The dewpoint temperature tdps is calculated using the August-Roche-Magnus approximation, based on tas and relative humidity (hurs) (Alduchov and Eskridge, 1996):

$$\mathrm{tdps} = \mathrm{B} \cdot \frac{\log\left(\frac{hurs}{100}\right) + \frac{\mathrm{A} \cdot \mathrm{tasC}}{\mathrm{B} + \mathrm{tasC}}}{\mathrm{A} - \log\left(\frac{\mathrm{hurs}}{100}\right) - \frac{\mathrm{A} \cdot \mathrm{tasC}}{\mathrm{B} + \mathrm{tasC}}} + 273.15 \ \ [\mathrm{K}] \tag{7}$$

where:

$$\mathrm{tasC} = \mathrm{tas} - 273.15 \tag{8}$$

$$\mathrm{A} = 17.625 \tag{9}$$

$$\mathrm{B} = 243.04 \tag{10}$$

Where surface pressure ps is not reported, the surface pressure is calculated based on the US standard atmosphere (National Oceanic and Atmospheric Administration et al., 1976), given pressure at sea level (psl), the temperature at the surface (tas) and the basin elevation h in the climate model grid.

$$ps = psl * \left(\frac{tas - h * L}{tas}\right)^{\frac{g * M_0}{R * L}} \ [Pa] \tag{11}$$

Where:

$$L = -0.0065 \ [K \ m^{-1}] \tag{12}$$

$$g = 9.80665 \ [m \ s^{-2}] \tag{13}$$

$$M_0 = 28.9644 \ \left[\frac{kg}{kmol}\right] \tag{14}$$

$$R = 8.31432 * 10^3 \ \left[\frac{N \cdot m}{kmol \cdot K}\right] \tag{15}$$

To derive the basin elevation h, first the MERIT digital elevation model (Hengl, 2018; Yamazaki et al., 2017) was reprojected to the coordinate system and resolution of each climate model grid, then the elevation was extracted using the basin polygons.

The near-surface wind speed (sfcWind) is calculated from the eastward and northward components (uas and vas):

$$\mathrm{sfcWind} = \sqrt{\mathrm{uas}^2 + \mathrm{vas}^2} \ [m \ s^{-1}] \tag{16}$$

Although uas and vas are included in some of the observed meteorological datasets (eg. ERA5-Land), bias correcting these variables presents a problem. Wind speed is best treated as a ratio variable for bias correction (Cannon, 2018), but uas and vas can have negative and positive values, which would require treating them as interval variables. This would preserve absolute changes in wind speed from the climate models, regardless of whether a specific catchment is generally windier or calmer than the wind speed from the climate model. Bias correcting the wind speed magnitude as a ratio variable, and thus preserving relative changes in wind speed, is thus preferable.

https://doi.org/10.5194/essd-2026-350
Preprint. Discussion started: 11 June 2026

Open Access Earth System Science Data Discussions

The Penman-Monteith Evapotranspiration (petfao56) is calculated using the FAO-56 formulation (Allen et al., 1998) by adapting code from (Singer et al., 2021):

$$\text{petfao56} = \frac{\left(\frac{\Delta}{\lambda} * (\text{rNet} - \text{G}) + \gamma * \left(\frac{900}{\text{tas}}\right) * \text{sfcWind.2m} * \frac{\text{vpSat}}{10^3} * \text{hurs}\right)}{\Delta + \gamma * (1 + 0.34 * \text{sfcWind.2m})} \; [\text{mm day}^{-1}] \quad (17)$$

Where:

$$\lambda = 2.45 \text{ MJ kg}^{-1} \quad (18)$$

is the latent heat of vaporization at 20°C.

$$\gamma = \frac{1.013 * 10^{-3} * \text{ps}}{0.622 * \lambda} \quad (19)$$

is the psychrometric constant at pressure ps.

$$\Delta = \frac{4098 * \text{vpSat}}{(\text{tasC} + 237.3)^2} \quad (20)$$

is the slope of the saturation vapour pressure curve.

$\text{G} = 0$ is the soil heat flux, assumed to be zero following equation 42 in (Allen et al., 1998).

$$\text{sfcWind.2m} = \text{sfcWind} * \frac{4.87}{\log(67.8 * 10 - 5.42)} \quad (21)$$

is the wind speed at 2m above the surface in m s^{-1}.

$$\text{vpSat} = 610.8 * \exp\left(\frac{(17.27 * \text{tasC})}{\text{tasC} + 237.3}\right) \quad (22)$$

is the saturation vapour pressure in Pa.

$$\text{rNet} = (\text{rss} + \text{rls}) * 86400 \left[\frac{\text{s}}{\text{day}}\right] * 10^{-6} \left[\frac{\text{MJ}}{\text{J}}\right] \quad (23)$$

is the sum of shortwave and longwave radiation in MJ m^{-2}:

Hargreaves' potential evapotranspiration is calculated according to the formula provided by Hargreaves and Samani, (1985):

$$\text{petharg} = 0.0023 * \text{RA} * (\text{tasmax} - \text{tasmin})^{0.5} * (\text{tasC} + 17.8) \quad (24)$$

Where tasmax, tasmin, and tasC are defined above and RA is the extraterrestrial radiation, calculated based on latitude, according to equations 21-25 in Allen et al., (1998).

Priestly-Taylor potential evapotranspiration is calculated using the same formula as (Miralles et al., 2011), which is the dataset used for CAMELS-IND (Mangukiya et al., 2025):

$$\text{petpriestly} = \frac{1}{\lambda} * \alpha * \frac{\Delta}{\Delta + \gamma} * (\text{rNet} - \text{G}) \; [\text{mm day}^{-1}] \quad (25)$$

I assume $\text{G} = 0$ and $\alpha = 1$, while Miralles et al. (2011) set α to either 0.8 or 1.26 and set G to a fraction of rNet, both depending on land cover. The bias correction that I apply to petpriestly will correct for the scaling differences that arise from differences in α and G.

Morton's point potential evapotranspiration, wet-environment potential evapotranspiration, and areal actual evapotranspiration are calculated according to the procedure outlined by Morton (1983) as modified by Zajaczkowski and

https://doi.org/10.5194/essd-2026-350
Preprint. Discussion started: 11 June 2026


Open Access Earth System Science Data Discussions

Jeffrey (2020) for the Scientific Information for Land Owners dataset used by CAMELS-AUS-v2 (Fowler et al., 2025). However, Zajaczkowski and Jeffrey (2020) calculated net radiation using cloud oktas, sunshine hours duration, and extraterrestrial radiation. Since I did not download cloud cover variables the CMIP6 models, I calculated net radiation as the sum of shortwave and longwave radiation.

2.3.2 Computational resources

Bias-correction was the most computationally expensive portion of this project. Overall, the project consumed approximately 2300 CPU-core-days, distributed over four high-performance computing centres maintained by the Digital Research Alliance of Canada. Because of the relatively large size of the datasets, the project also required a large amount of working memory (846 TB-days). Based on CPU-core-equivalent days (which track both CPU and memory usage), I estimate this project is responsible for approximately 1.7 tonnes of CO_2-equivalent emissions, or a little over two round-trip flights from New York to London. See Appendix C for details.

3 Preservation of changes in means and extreme values

Quantile delta mapping is designed to preserve the changes (deltas) in median and extreme values predicted in climate models (Cannon et al., 2015). For interval quantities absolute deltas are preserved (*e.g.,* degrees Celsius), while for ratio quantities relative deltas are preserved (*e.g.,* percentage change in precipitation). However, if the seasonality of a particular variable is not well simulated by the climate model, changes in extreme values in the bias corrected time series can be different from the changes predicted by the climate model. This occurs because the bias correction is applied to individually to each half month. The change in extreme values in the bias-corrected data will thus reflect the delta calculated for the period of the year for which the observed maximum occurs, not the delta for which the simulated maximum occurs. In addition, if a variable's modelled and observed distributions differ very much then changes in the mean can be imperfectly preserved.

I investigated how well the bias-correction preserves the changes in the climate model. For each ensemble member and catchment, I calculated the mean and 10-year return period minimum and maximum for the reference period (1981-2010) and the 30-year period corresponding to 3ºC above preindustrial conditions. For the return levels I used a block maxima/minima approach, with a block size of one year. The 10-year return period value was estimated empirically as the third highest (or lowest) value in each 30-year period. This is done for simplicity and interpretability of the results. I then calculate the change between the reference and future period, and compare these changes calculated for the raw climate model output and for the bias-corrected dataset.

Figure 2 shows a comparison of the raw and bias-corrected (QDM) change in the mean and 10-year return period maximum values for the four ratio variables, for all climate models and all catchments within the Caravan dataset. Figure 3 shows the same comparison, for the mean and 10-year return period minimum and maximum values, for the interval variables.

https://doi.org/10.5194/essd-2026-350
Preprint. Discussion started: 11 June 2026


Open Access Earth System Science Data Discussions

Overall, I find that mean changes are well preserved across all variables. Changes in precipitation are the least well preserved (the boxplots in the first panel of Fig. 2 show the widest distribution). This occurs because the distribution of modelled precipitation often differs significantly from the observed distribution. Changing each quantile of the bias-corrected distribution by the same factor as each quantile of the raw distribution thus does not produce an identical change in the mean. Nevertheless, the QDM change ratio is within 10% of the raw change ratio over 98% of the time, and within 20% over 99.8% of the time.

Changes in extreme values (10-year return period minimum and maximum values) are less well preserved than changes in the mean. In particular, where the climate models predict reductions in 10-year return period precipitation, maximum temperature, and longwave radiation, the bias-corrected data may not fully reflect these reductions. Nevertheless, for the vast majority of cases, the bias-corrected changes in extreme values are similar to the changes in the raw model output.

https://doi.org/10.5194/essd-2026-350
Preprint. Discussion started: 11 June 2026

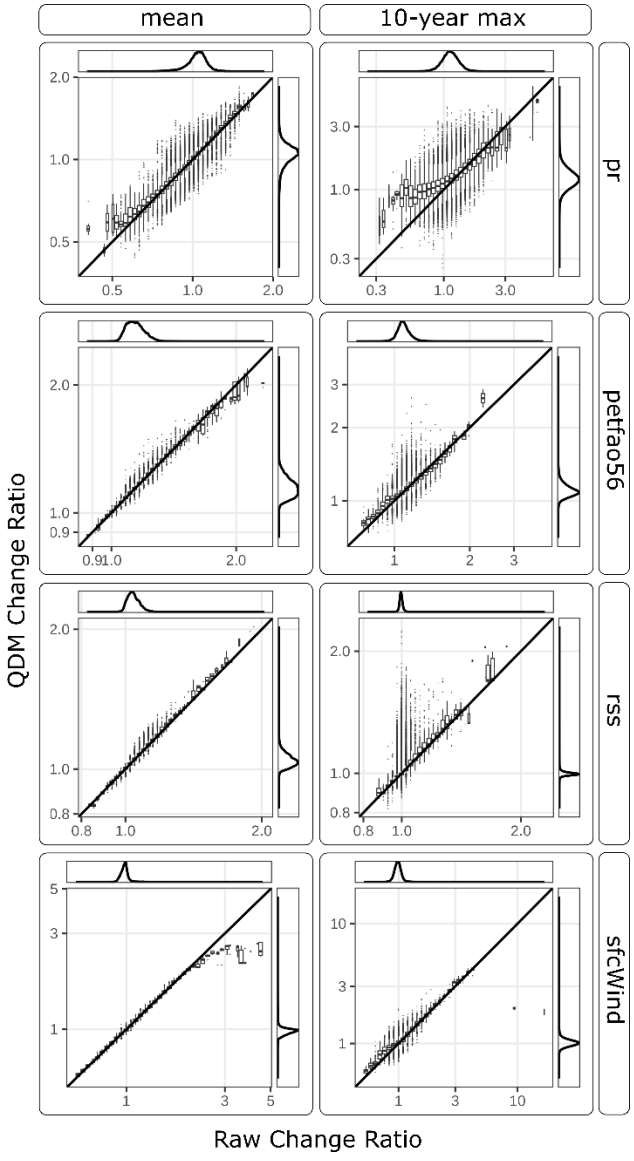

Figure 2: Preservation of relative changes in the four ratio variables by Quantile Delta Mapping. The changes compare values at 3ºC with values during the reference period (1981-2010). The first column shows changes in mean quantities, and the second column shows changes in the 10-year return period maximum.

https://doi.org/10.5194/essd-2026-350
Preprint. Discussion started: 11 June 2026

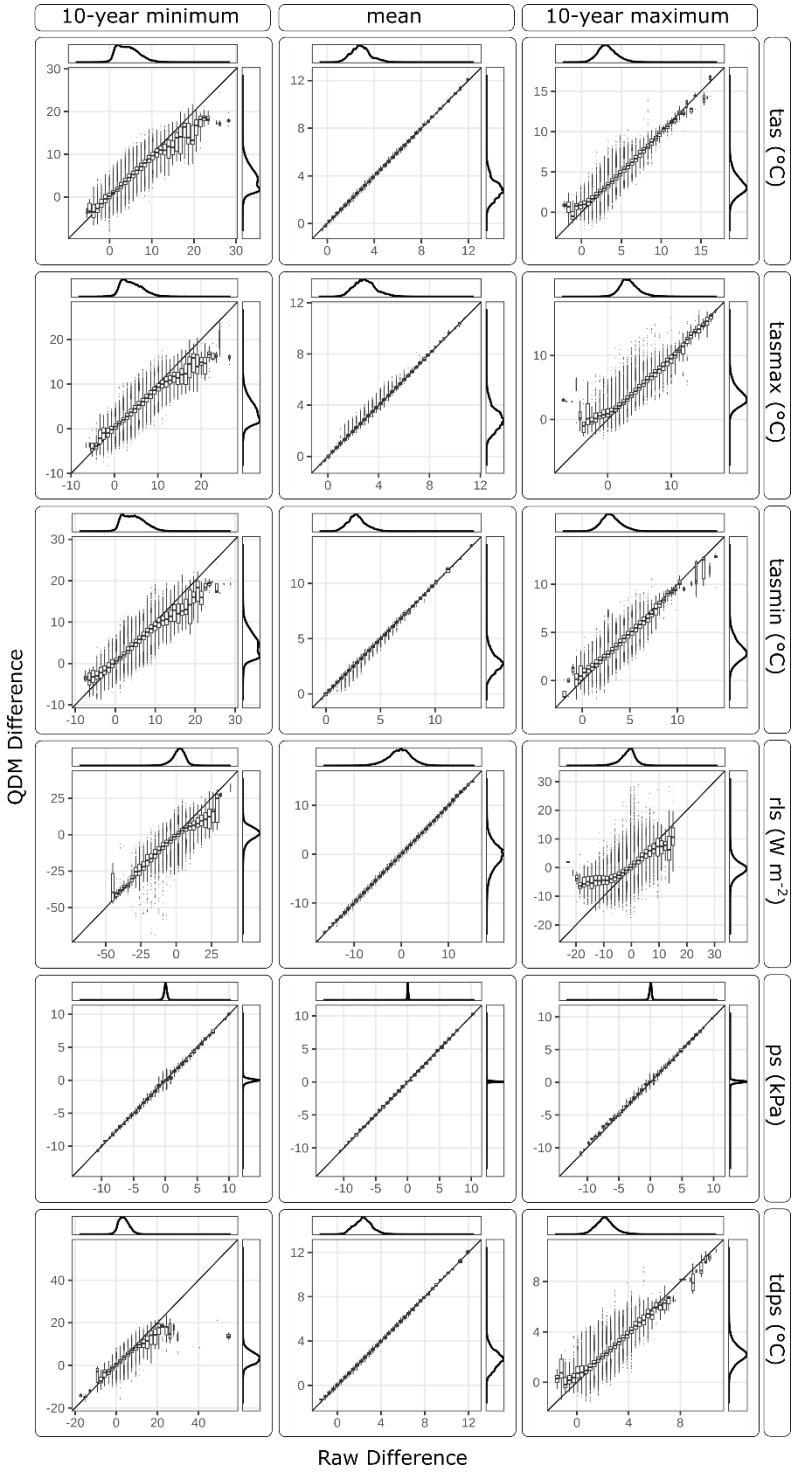

Figure 3: Preservation of absolute changes in the six interval variables by Quantile Delta Mapping. The changes compare values at 3ºC with values during the reference period (1981-2010). The middle column shows changes in mean quantities, and the first and third columns show changes in the 10-year return period minimum and maximum, respectively.

https://doi.org/10.5194/essd-2026-350
Preprint. Discussion started: 11 June 2026

4 Predicted changes in hydrometeorological extremes

I present some projections of changes in precipitation and evapotranspiration extremes using the bias-corrected data from the Caravan dataset for a warming of 3ºC above preindustrial conditions (the first method described in Section 2.1). I choose to analyse precipitation events with a 10-year return period as well as the minimum 12-month Standardized Precipitation Evapotranspiration Index (SPEI) observed in a 30-year period (Vicente-Serrano et al., 2010).

Figure 4 shows the projected change in 10-year return period single-day precipitation ($pr_{24,10}$). For each ensemble member, I calculated the maximum daily precipitation for each year in the normal period (1981-2010) and for the projection period (30 years in SSP 5-8.5 for which the average global warming level is 3ºC above preindustrial conditions). For each 30-year period, I calculate $pr_{24,10}$ as the precipitation amount that is met or exceeded in 3 of 30 years. I then calculate the change ratio between the reference and projection periods and average this ratio across all variants of each climate model, and then across the 12 climate models.

Extreme precipitation is projected to increase almost everywhere. Only 30 of the 24870 catchments in the Caravan dataset show a decrease in 10-year precipitation amounts, based on the ensemble mean; most of these catchments are located in Chile and Puerto Rico. Increases of greater than 30% are projected in 27% of catchments, located on all continents. However, there is considerable variability between different climate models on which regions will see the largest changes.

Figure 5 shows the projected minimum (most extreme) SPEI under 3ºC of warming. For each ensemble member I calibrated the 12-month SPEI (SPEI-12) based on the reference period and then calculated the SPEI values for the projection period. For the ensemble mean I averaged the minimum projected SPEI-12 across all variants of each climate model and then across climate models.

Among the catchments currently included in the Caravan dataset, regions that are predicted to see the most extreme SPEI values (<-5) include the Amazon River basin and the southern Dead Sea basin. Under the normality and stationarity assumptions of the SPEI, values less than -5 would be expected to occur less than once in 3 million years. These projections are quite robust across the 12 climate models, with all models predicting minimum SPEI values of -3 or less in these two basins. These extreme drying regions agree with the results presented by Bhardwaj et al., (2025) who predicted extreme drying across much of Brazil and most of North Africa and the Arabian peninsula.

SPEI values less than -4 (a return period of ~30,000 years) are also expected to occur in northern Spain, parts of the western Great Plains and Rocky Mountains of the United States, southern Mexico the upper Okavango and Zambezi Basins, the Western Cape of South Africa, and southwestern Australia.

https://doi.org/10.5194/essd-2026-350
Preprint. Discussion started: 11 June 2026

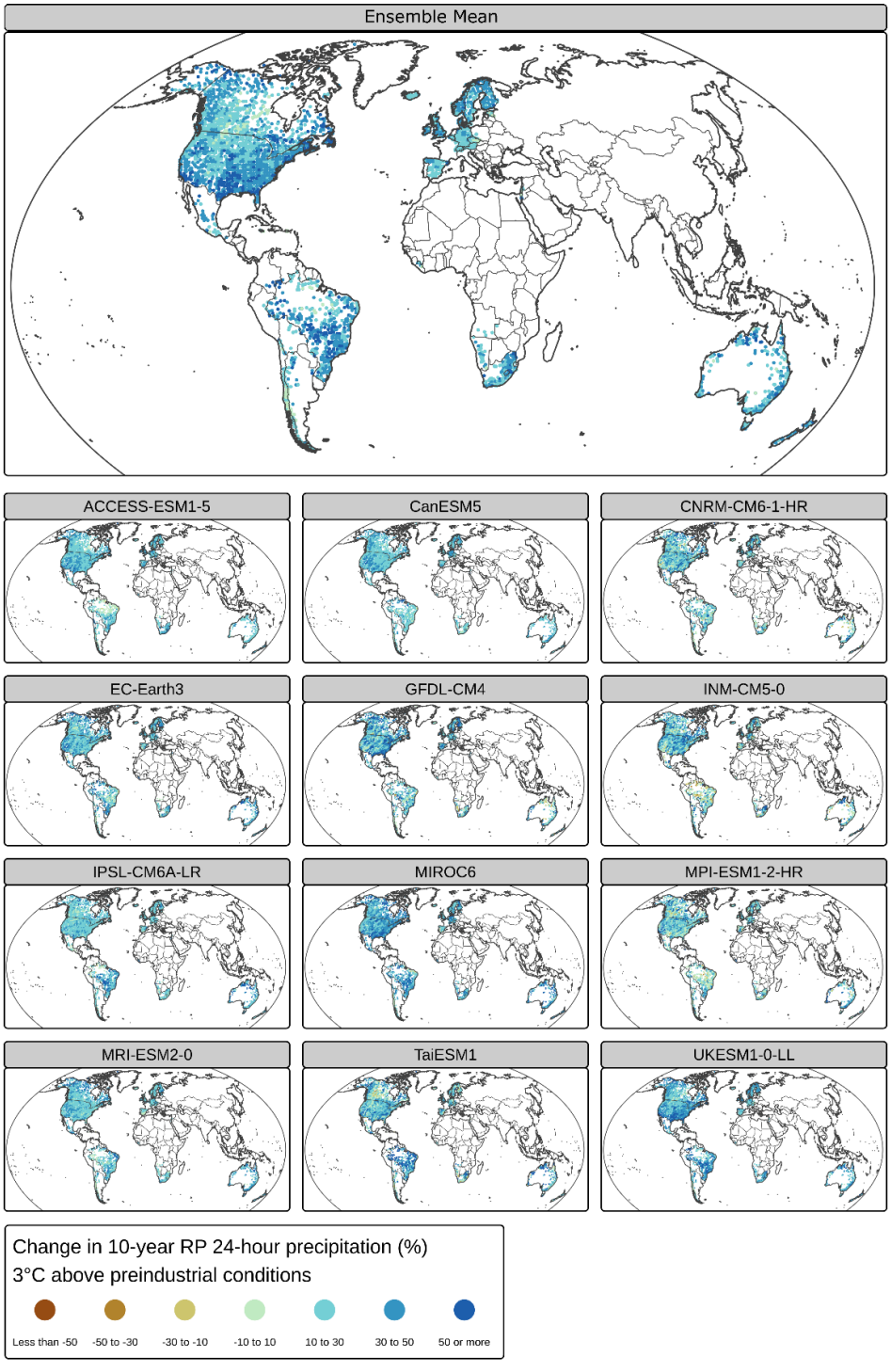

315 **Figure 4: Projected change in 10-year return period 24-hour precipitation total, for global warming of 3ºC above preindustrial conditions, relative to 1981-2010.**

https://doi.org/10.5194/essd-2026-350
Preprint. Discussion started: 11 June 2026

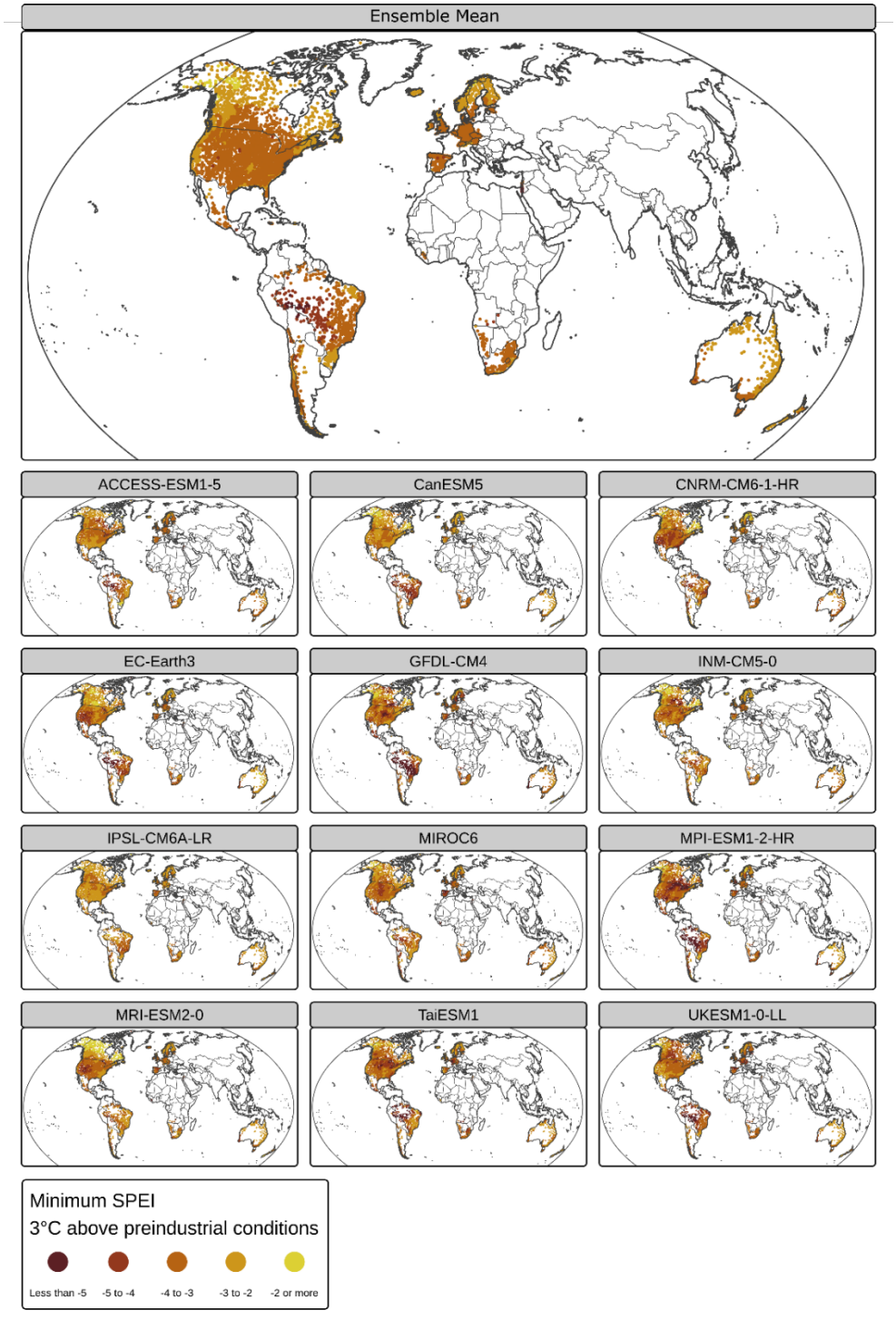

Figure 5: Minimum SPEI for a 30-year period with an average global warming of 3°C. The SPEI is calibrated to the reference period (1981-2010).

https://doi.org/10.5194/essd-2026-350
Preprint. Discussion started: 11 June 2026

5 Conclusions and Limitations

Climate change is profoundly altering streamflow around the world, with effects on aquatic ecosystems, hydropower, and water security. Projections of streamflow under climate change scenarios can inform climate adaptation strategies as well as provide support for emissions reductions to limit the worst impacts. This study introduces Caravan-CMIP6, which provides opportunities to project climate impacts using already-available large-sample hydrometeorological datasets.

Caravan-CMIP6 provides a great breadth of data, across many catchments, variables, and climate models. However, as a general-purpose bias-corrected dataset, it has some limitations that were required to keep the dataset size and computational requirements reasonable. First, no climate model within our dataset contributes more than 10 ensemble members. Users interested in performing Single-Model Initial Condition Large Ensembles (Deser et al., 2020) may be able to gain some insight by using the two climate models with 10 ensemble members each (CanESM5 and ACCESS-ESM1-5) but should be aware that many more runs of these models are available. Many more models are also available too, which could not be included in this dataset because they did not report all the necessary variables.

Second, I used a robust but simple statistical bias-correction algorithm. Dynamical downscaling and bias correction can provide more realistic meteorological fields for regional studies. Multivariate statistical bias correction algorithms are also available, which preserve the relationships between variables; however, these are approximately an order of magnitude more computationally expensive and were thus ruled out.

Lastly, the distribution of catchments provided in Caravan-CMIP6 is quite biased towards Europe and North America. I ensured that I included new datasets from locations that have been less well-represented in the large-sample hydrologic literature (*e.g.* CAMELS-IND and CAMELS-COL) but even so, there are no catchments included for most countries in Asia, Africa, or Oceania. These regions may exhibit unique responses to climate change that cannot be studied by using large-sample hydrologic datasets from Europe and North America.

6 Data availability

The Caravan-CMIP6 dataset described in this study is available at https://doi.org/10.20383/103.01644 (Ruzzante, 2026). This includes the raw and bias-corrected meteorological variables for catchments in all ten LSH datasets. Additionally, the bias-corrected data for Caravan are available in analysis-ready zarr format in the Google Cloud Platform. An example of how to access these data is provided in the GitHub repository: https://github.com/sruzzante/Caravan-CMIP6/.

The raw climate model data in raster format is available from the Earth System Grid Foundation (https://esgf.github.io/nodes.html). The basin shapefiles and observed meteorological forcings are available from each respective LSH dataset: CAMELS: https://doi.org/10.5065/D6MW2F4D (Addor et al., 2017; Newman et al., 2015), CAMELS-AUS-v2 : https://doi.org/10.5194/essd-17-4079-2025 (Fowler et al., 2025), CAMELS-BR: https://doi.org/10.5281/zenodo.3709337 (Chagas et al., 2020), CAMELS-CH: https://doi.org/10.5194/essd-15-5755-2023 (Höge et al., 2023), CAMELS-CL: https://doi.org/10.5194/hess-22-5817-2018 (Alvarez-Garreton et al., 2018), CAMELS-

https://doi.org/10.5194/essd-2026-350
Preprint. Discussion started: 11 June 2026

COL: https://doi.org/10.5194/essd-2025-200 (Jimenez et al., 2025), CAMELS-DE: https://doi.org/10.5194/essd-16-5625-2024 (Loritz et al., 2024), CAMELS-GB-v2: https://doi.org/10.5194/essd-2025-608 (Coxon et al., 2025), CAMELS-IND: https://doi.org/10.5194/essd-17-461-2025 (Mangukiya et al., 2025), Caravan: https://doi.org/10.1038/s41597-023-01975-w (Addor et al., 2017; Alvarez-Garreton et al., 2018; Arsenault et al., 2020; Chagas et al., 2025; Coxon et al., 2020; Fowler et al., 2025; Klingler et al., 2021; Kratzert et al., 2023; Newman et al., 2015), and the extensions to Caravan: https://github.com/kratzert/Caravan/discussions/10 (Casado Rodríguez, 2025; Czech Hydrometeorological Institute et al., 2025; Färber et al., 2025; Helgason and Nijssen, 2024; Höge et al., 2023; Koch et al., 2025; Loritz et al., 2024; Morin, 2025). The MERIT digital elevation model is available at https://doi.org/10.5281/zenodo.1447209.

7 Code availability

The codes developed to extract the raw climate model data, calculate the required variables, perform the quantile delta mapping, and save the data to its final format are provided at http://www.github.com/sruzzante/Caravan-CMIP6. The codes rely most heavily on the terra and MBC packages for R (Cannon, 2024a; Hijmans et al., 2026).

Appendix A: Miscellaneous notes:

UKESM1-0-LL: Users should be aware that UKES1-0-LL uses a 360-day calendar, in which each month has 30 days. Dates such as February 30 are valid in this calendar, and I recommend using the CFtime packages in R (Laake, 2025) and cftime and nc-time-axis in python (nc-time-axis contributors, 2026; Whitaker et al., 2025).

In addition, the UKESM1-0-LL raw raster data contains unrealistic spikes in tasmax for some grid cells and days, with very high daily maximum temperatures (tasmax). This is probably a result of non-physical inefficient mixing by the model's sub-grid scale mixing scheme, and is a known error: https://errata.ipsl.fr/static/view.html?uid=76b3f818-d65f-c76b-bfd8-cae5bc27825c, for which the recommended solution is to mask out values above 335K prior to analysis. I wanted to avoid missing values in the time series, so I instead replaced all grid cells with tasmax>335K with the value 2*tas-tasmin, under the assumption that the maximum and minimum temperatures are equidistant from the mean.

CAMELS: The variables labelled as maximum and minimum temperature (tmax (C). and tmin (C)) in the CAMELS dataset (Newman et al., 2015) for the NLDAS and Maurer forcings are in fact the mean temperature. The CMIP6 mean temperature *tas* was accordingly bias-corrected to match the variable labelled as tmax (C). I label these variables tmean.C.maurer and tmean.C.nldas.

Also, note that the solar radiation variable in CAMELS is averaged over the daylight period of the day. For the bias correction, I converted this variable to be averaged over 24 hours, performed the bias correction, and then converted back to a daylight-period average. I provide the daylight period as dayl.s. in the bias-corrected data, but note that no correction is made to this variable

https://doi.org/10.5194/essd-2026-350
Preprint. Discussion started: 11 June 2026

CAMELS-CH: The meteorological data begin at 1981-10-01, so I used a reference period of 1981-10-01 to 2011-09-30 for this dataset.

Caravan: For the CAMELS-ES extension the meteorological data are provided only from 1990. I re-extracted the ERA5-Land data using the codes provided by Kratzert et al., 2023) .

Appendix B: Variable Definitions

Where possible I adopt the CMIP6 conventions for variable abbreviations and units (https://clipc-services.ceda.ac.uk/dreq/index/var.html).

Table B1: Variable Definitions

Variable	Long Name	Units	CMIP6 variable?
tas	Near-surface air temperature (usually 2 m)	K	yes
tasmax	Near-surface maximum daily air temperature (usually 2 m)	K	yes
tasmin	Near-surface maximum daily air temperature (usually 2 m)	K	yes
tasC	Near-surface air temperature (usually 2 m) in Celsius	ºC	no
hurs	Near-surface relative humidity	%	yes
pr	Precipitation	kg m^{-2} s^{-1}	yes
ps	Surface air pressure	Pa	yes
psl	Sea level pressure	Pa	yes
rlds	Surface downwelling longwave radiation	W m^{-2}	yes
rlus	Surface upwelling longwave radiation	W m^{-2}	yes
rls	Net longwave surface radiation (downwards)	W m^{-2}	yes
rsds	Surface downwelling shortwave radiation	W m^{-2}	yes
rsus	Surface upwelling shortwave radiation	W m^{-2}	yes
rss	Net shortwave surface radiation (downwards)	W m^{-2}	yes
rNet	Net shortwave + longwave radiation (downwards)	W m^{-2}	no
uas	Eastward near-surface wind (10 m)	m s^{-1}	yes
vas	Northward near-surface wind (10 m)	m s^{-1}	yes
sfcWind	Near-surface wind speed (10 m)	m s^{-1}	yes
tdps	2 m dewpoint temperature	K	yes

https://doi.org/10.5194/essd-2026-350
Preprint. Discussion started: 11 June 2026

Open Access Earth System Science Data Discussions

vp	Water vapour pressure	Pa	no
vpDeficit	Water vapour pressure deficit	Pa	no
vpSat	Saturation water vapour pressure	Pa	no
petfao56	Potential evapotranspiration calculated using the FAO-56 Penman-Monteith formula (Allen et al., 1998)	kg m^{-2} day^{-1}	no
petharg	Potential evapotranspiration calculated using the Hargreaves formula (Hargreaves and Samani, 1985)	kg m^{-2} day^{-1}	no
petpriestly	Potential evapotranspiration calculated using the Priestly-Taylor formula (Priestley and Taylor, 1972)	kg m^{-2} day^{-1}	no
et_morton_potential	Potential (point) evapotranspiration calculated using the Morton formula (Morton, 1983)	kg m^{-2} day^{-1}	no
et_morton_actual	Areal actual evapotranspiration calculated using the Morton formula (Morton, 1983)	kg m^{-2} day^{-1}	no
et_morton_wet	Wet environment areal potential evapotranspiration calculated using the Morton formula (Morton, 1983)	kg m^{-2} day^{-1}	no

Appendix C: Computational resources and CO_2-equivalent calculation

I tracked the total CPU-core-days and CPU-equivalent-core-days used for this project, across four high-performance computing (HPC) cluster (Fir, Narval, Nibi, and Rorqual). I estimated the power efficiency in [kW/core] of each cluster using published power consumption and total number of cores for each HPC (Graham and Jake Hirsch-Allen, 2024; University of Waterloo, 2017). I multiplied the CPU-equivalent-core-hours by the power efficiency to calculate total energy consumption in kWh. I then multiplied this value by the carbon intensity of each provincial grid (Environment and Climate Change Canada, 2025; annex 13) to calculate total CO_2-equivalent emissions.

Table C1: Calculation of energy usage and CO_2-equivalent emissions

HPC cluster	CPU-core-days used	CPU-equivalent-core-days used	Power Efficiency (kW/core)	Total Energy used (kWh)	Carbon intensity (g CO_2-eq/kWh)	Total CO_2-eq (kg)
Fir	1459	123140	0.012	34633	18	623

https://doi.org/10.5194/essd-2026-350
Preprint. Discussion started: 11 June 2026

Narval	445	25591	0.004	2502	1.9	5
Nibi	275	38136	0.020	18027	59	1063
Rorqual	183	29580	0.003	2350	1.9	5

Competing interests

I declare I have no competing interests.

Acknowledgements

This work was enabled in part by support provided by the Digital Research Alliance of Canada, including the BC DRI group, Calcul Québec, and Compute Ontario.

I thank Grey Nearing for help securing Google Cloud Storage for this dataset.

AI tools (ChatGPT and Claude) were used to support some coding tasks in this study. No AI was used in the manuscript writing.

References

Addor, N., Newman, A. J., Mizukami, N., and Clark, M. P.: The CAMELS data set: catchment attributes and meteorology for large-sample studies, Hydrology and Earth System Sciences, 21, 5293–5313, https://doi.org/10.5194/hess-21-5293-2017, 2017.

Alduchov, O. A. and Eskridge, R. E.: Improved Magnus Form Approximation of Saturation Vapor Pressure, Journal of Applied Meteorology, 35, 601–609, https://doi.org/10.1175/1520-0450(1996)035%253C0601:IMFAOS%253E2.0.CO;2, 1996.

Allen, R. G., Pereira, L. S., Raes, D., and Smith, M.: Crop evapotranspiration: guidelines for computing crop water requirements, Food and Agriculture Organization of the United Nations, Rome, 300 pp., 1998.

Alvarez-Garreton, C., Mendoza, P. A., Boisier, J. P., Addor, N., Galleguillos, M., Zambrano-Bigiarini, M., Lara, A., Puelma, C., Cortes, G., Garreaud, R., McPhee, J., and Ayala, A.: The CAMELS-CL dataset: catchment attributes and meteorology for large sample studies – Chile dataset, Hydrology and Earth System Sciences, 22, 5817–5846, https://doi.org/10.5194/hess-22-5817-2018, 2018.

Arsenault, R., Brissette, F., Martel, J.-L., Troin, M., Lévesque, G., Davidson-Chaput, J., Gonzalez, M. C., Ameli, A., and Poulin, A.: A comprehensive, multisource database for hydrometeorological modeling of 14,425 North American watersheds, Sci Data, 7, 243, https://doi.org/10.1038/s41597-020-00583-2, 2020.

Arsenault, R., Martel, J.-L., Brunet, F., Brissette, F., and Mai, J.: Continuous streamflow prediction in ungauged basins: long short-term memory neural networks clearly outperform traditional hydrological models, Hydrology and Earth System Sciences, 27, 139–157, https://doi.org/10.5194/hess-27-139-2023, 2023.

https://doi.org/10.5194/essd-2026-350
Preprint. Discussion started: 11 June 2026

Berghuijs, W. R., Hale, K., and Beria, H.: Technical note: Streamflow seasonality using directional statistics, Hydrology and Earth System Sciences, 29, 2851–2862, https://doi.org/10.5194/hess-29-2851-2025, 2025.

Bevacqua, E., Fischer, E., Sillmann, J., and Zscheischler, J.: Moderate global warming does not rule out extreme global climate outcomes, Nature, 651, 946–953, https://doi.org/10.1038/s41586-026-10237-9, 2026.

Bhardwaj, K., Mishra, A., and Khedun, C. P.: Global droughts in a warming climate: Evaluation of SPI and SPEI under 1.5°, 2°, and 3 °C global warming, Journal of Hydrology, 659, 133309, https://doi.org/10.1016/j.jhydrol.2025.133309, 2025.

Boucher, O., Servonnat, J., Albright, A. L., Aumont, O., Balkanski, Y., Bastrikov, V., Bekki, S., Bonnet, R., Bony, S., Bopp, L., Braconnot, P., Brockmann, P., Cadule, P., Caubel, A., Cheruy, F., Codron, F., Cozic, A., Cugnet, D., D'Andrea, F., Davini, P., de Lavergne, C., Denvil, S., Deshayes, J., Devilliers, M., Ducharne, A., Dufresne, J.-L., Dupont, E., Éthé, C., Fairhead, L., Falletti, L., Flavoni, S., Foujols, M.-A., Gardoll, S., Gastineau, G., Ghattas, J., Grandpeix, J.-Y., Guenet, B., Guez, E., Lionel, Guilyardi, E., Guimberteau, M., Hauglustaine, D., Hourdin, F., Idelkadi, A., Joussaume, S., Kageyama, M., Khodri, M., Krinner, G., Lebas, N., Levavasseur, G., Lévy, C., Li, L., Lott, F., Lurton, T., Luyssaert, S., Madec, G., Madeleine, J.-B., Maignan, F., Marchand, M., Marti, O., Mellul, L., Meurdesoif, Y., Mignot, J., Musat, I., Ottlé, C., Peylin, P., Planton, Y., Polcher, J., Rio, C., Rochetin, N., Rousset, C., Sepulchre, P., Sima, A., Swingedouw, D., Thiéblemont, R., Traore, A. K., Vancoppenolle, M., Vial, J., Vialard, J., Viovy, N., and Vuichard, N.: Presentation and Evaluation of the IPSL-CM6A-LR Climate Model, Journal of Advances in Modeling Earth Systems, 12, e2019MS002010, https://doi.org/10.1029/2019MS002010, 2020.

Brunner, M. I., Mittermeier, M., Anderson, B., Büeler, D., and Muñoz-Castro, E.: Spatially Compounding Drought-Flood Events Are Favored by Atmospheric Blocking Over Europe, Water Resources Research, 61, e2024WR039622, https://doi.org/10.1029/2024WR039622, 2025.

Cannon, A. J.: Multivariate quantile mapping bias correction: an N-dimensional probability density function transform for climate model simulations of multiple variables, Clim Dyn, 50, 31–49, https://doi.org/10.1007/s00382-017-3580-6, 2018.

Cannon, A. J.: MBC: Multivariate Bias Correction of Climate Model Outputs, , https://doi.org/10.32614/CRAN.package.MBC, 2024a.

Cannon, A. J.: The Impact of "Hot Models" on a CMIP6 Ensemble Used by Climate Service Providers in Canada: Do Global Constraints Lead to Appreciable Differences in Regional Projections?, Journal of Climate, 37, 2141–2154, https://doi.org/10.1175/JCLI-D-23-0459.1, 2024b.

Cannon, A. J., Sobie, S. R., and Murdock, T. Q.: Bias Correction of GCM Precipitation by Quantile Mapping: How Well Do Methods Preserve Changes in Quantiles and Extremes?, Journal of Climate, 28, 6938–6959, https://doi.org/10.1175/JCLI-D-14-00754.1, 2015.

Cannon, A. J., Alford, H., Shrestha, R. R., Kirchmeier-Young, M. C., and Najafi, M. R.: Canadian Large Ensembles Adjusted Dataset version 1 (CanLEADv1): Multivariate bias-corrected climate model outputs for terrestrial modelling and attribution studies in North America, Geoscience Data Journal, 9, 288–303, https://doi.org/10.1002/gdj3.142, 2022.

Casado Rodríguez, J.: CAMELS-ES: Catchment Attributes and Meteorology for Large-Sample Studies – Spain, https://doi.org/10.5281/zenodo.15040948, 2025.

Castaneda-Gonzalez, M., Poulin, A., Romero-Lopez, R., and Turcotte, R.: Hydrological models weighting for hydrological projections: The impacts on future peak flows, Journal of Hydrology, 625, 130098, https://doi.org/10.1016/j.jhydrol.2023.130098, 2023a.

https://doi.org/10.5194/essd-2026-350
Preprint. Discussion started: 11 June 2026

Castaneda-Gonzalez, M., Poulin, A., Romero-Lopez, R., and Turcotte, R.: Weighting climate models for hydrological projections: effects on contrasting hydroclimatic regions, Climatic Change, 176, 170, https://doi.org/10.1007/s10584-023-03643-9, 2023b.

Cerveny, R. S., Lawrimore, J., Edwards, R., and Landsea, C.: Extreme Weather Records, Bulletin of the American Meteorological Society, 88, 853–860, https://doi.org/10.1175/BAMS-88-6-853, 2007.

Chagas, V. B. P., Chaffe, P. L. B., Addor, N., Fan, F. M., Fleischmann, A. S., Paiva, R. C. D., and Siqueira, V. A.: CAMELS-BR: hydrometeorological time series and landscape attributes for 897 catchments in Brazil, Earth System Science Data, 12, 2075–2096, https://doi.org/10.5194/essd-12-2075-2020, 2020.

Chagas, V. B. P., Chaffe, P. L. B., Addor, N., Fan, F. M., Fleischmann, A. S., Paiva, R. C. D., and Siqueira, V. A.: CAMELS-BR: Hydrometeorological time series and landscape attributes for 897 catchments in Brazil - link to files. (1.2), https://doi.org/10.5281/zenodo.15025488, 2025.

Chen, J., Shi, X., Gu, L., Wu, G., Su, T., Wang, H.-M., Kim, J.-S., Zhang, L., and Xiong, L.: Impacts of climate warming on global floods and their implication to current flood defense standards, Journal of Hydrology, 618, 129236, https://doi.org/10.1016/j.jhydrol.2023.129236, 2023.

Coxon, G., Addor, N., Bloomfield, J. P., Freer, J., Fry, M., Hannaford, J., Howden, N. J. K., Lane, R., Lewis, M., Robinson, E. L., Wagener, T., and Woods, R.: CAMELS-GB: hydrometeorological time series and landscape attributes for 671 catchments in Great Britain, Earth System Science Data, 12, 2459–2483, https://doi.org/10.5194/essd-12-2459-2020, 2020.

Coxon, G., Zheng, Y., Barbedo, R., Cooper, H., Fileni, F., Fowler, H. J., Fry, M., Green, A., Gribbin, T., Harfoot, H., Lewis, E., Neto, G. G. R., Qiu, X., Salwey, S., and Wendt, D. E.: CAMELS-GB v2: hydrometeorological time series and landscape attributes for 671 catchments in Great Britain, Earth System Science Data Discussions, 1–44, https://doi.org/10.5194/essd-2025-608, 2025.

Czech Hydrometeorological Institute, Krejčí, J., and Nearing, G.: [CAMELS-CZ] Catchment Attributes and Meteorology for Large-Sample Studies -- Czechia, https://doi.org/10.5281/zenodo.17769325, 2025.

Dallaire, G., Poulin, A., Arsenault, R., and Brissette, F.: Uncertainty of potential evapotranspiration modelling in climate change impact studies on low flows in North America, Hydrological Sciences Journal, 66, 689–702, https://doi.org/10.1080/02626667.2021.1888955, 2021.

Deser, C., Lehner, F., Rodgers, K. B., Ault, T., Delworth, T. L., DiNezio, P. N., Fiore, A., Frankignoul, C., Fyfe, J. C., Horton, D. E., Kay, J. E., Knutti, R., Lovenduski, N. S., Marotzke, J., McKinnon, K. A., Minobe, S., Randerson, J., Screen, J. A., Simpson, I. R., and Ting, M.: Insights from Earth system model initial-condition large ensembles and future prospects, Nat. Clim. Chang., 10, 277–286, https://doi.org/10.1038/s41558-020-0731-2, 2020.

Döscher, R., Acosta, M., Alessandri, A., Anthoni, P., Arsouze, T., Bergman, T., Bernardello, R., Boussetta, S., Caron, L.-P., Carver, G., Castrillo, M., Catalano, F., Cvijanovic, I., Davini, P., Dekker, E., Doblas-Reyes, F. J., Docquier, D., Echevarria, P., Fladrich, U., Fuentes-Franco, R., Gröger, M., v. Hardenberg, J., Hieronymus, J., Karami, M. P., Keskinen, J.-P., Koenigk, T., Makkonen, R., Massonnet, F., Ménégoz, M., Miller, P. A., Moreno-Chamarro, E., Nieradzik, L., van Noije, T., Nolan, P., O'Donnell, D., Ollinaho, P., van den Oord, G., Ortega, P., Prims, O. T., Ramos, A., Reerink, T., Rousset, C., Ruprich-Robert, Y., Le Sager, P., Schmith, T., Schrödner, R., Serva, F., Sicardi, V., Sloth Madsen, M., Smith, B., Tian, T., Tourigny, E., Uotila, P., Vancoppenolle, M., Wang, S., Wårlind, D., Willén, U., Wyser, K., Yang, S., Yepes-Arbós, X., and Zhang, Q.: The EC-Earth3 Earth system model for the Coupled Model Intercomparison Project 6, Geoscientific Model Development, 15, 2973–3020, https://doi.org/10.5194/gmd-15-2973-2022, 2022.

https://doi.org/10.5194/essd-2026-350
Preprint. Discussion started: 11 June 2026

Environment and Climate Change Canada: National Inventory Report 1990–2023: Greenhouse Gas Sources and Sinks in Canada, 2025.

Färber, C., Plessow, H., Mischel, S., Kratzert, F., Addor, N., Shalev, G., and Looser, U.: GRDC-Caravan: extending the original dataset with data from the Global Runoff Data Centre (0.5), https://doi.org/10.5281/zenodo.15124865, 2025.

Feng, D., Liu, J., Lawson, K., and Shen, C.: Differentiable, Learnable, Regionalized Process-Based Models With Multiphysical Outputs can Approach State-Of-The-Art Hydrologic Prediction Accuracy, Water Resources Research, 58, e2022WR032404, https://doi.org/10.1029/2022WR032404, 2022.

Feng, D., Beck, H., Lawson, K., and Shen, C.: The suitability of differentiable, physics-informed machine learning hydrologic models for ungauged regions and climate change impact assessment, Hydrology and Earth System Sciences, 27, 2357–2373, https://doi.org/10.5194/hess-27-2357-2023, 2023.

Fowler, K. J. A., Zhang, Z., and Hou, X.: CAMELS-AUS v2: updated hydrometeorological time series and landscape attributes for an enlarged set of catchments in Australia, Earth System Science Data, 17, 4079–4095, https://doi.org/10.5194/essd-17-4079-2025, 2025.

Graham, D. and Jake Hirsch-Allen: Can Canada Compute?, The Dais, 2024.

Hargreaves, G. H. and Samani, Z. A.: Reference Crop Evapotranspiration from Temperature, Applied Engineering in Agriculture, 1, 96–99, https://doi.org/10.13031/2013.26773, 1985.

Hausfather, Z., Marvel, K., Schmidt, G. A., Nielsen-Gammon, J. W., and Zelinka, M.: Climate simulations: recognize the 'hot model' problem, Nature, 605, 26–29, https://doi.org/10.1038/d41586-022-01192-2, 2022.

Held, I. M., Guo, H., Adcroft, A., Dunne, J. P., Horowitz, L. W., Krasting, J., Shevliakova, E., Winton, M., Zhao, M., Bushuk, M., Wittenberg, A. T., Wyman, B., Xiang, B., Zhang, R., Anderson, W., Balaji, V., Donner, L., Dunne, K., Durachta, J., Gauthier, P. P. G., Ginoux, P., Golaz, J.-C., Griffies, S. M., Hallberg, R., Harris, L., Harrison, M., Hurlin, W., John, J., Lin, P., Lin, S.-J., Malyshev, S., Menzel, R., Milly, P. C. D., Ming, Y., Naik, V., Paynter, D., Paulot, F., Ramaswamy, V., Reichl, B., Robinson, T., Rosati, A., Seman, C., Silvers, L. G., Underwood, S., and Zadeh, N.: Structure and Performance of GFDL's CM4.0 Climate Model, Journal of Advances in Modeling Earth Systems, 11, 3691–3727, https://doi.org/10.1029/2019MS001829, 2019.

Helgason, H. B. and Nijssen, B.: LamaH-Ice: LArge-SaMple DAta for Hydrology and Environmental Sciences for Iceland, Earth System Science Data, 16, 2741–2771, https://doi.org/10.5194/essd-16-2741-2024, 2024.

Hengl, T.: Global DEM derivatives at 250 m, 1 km and 2 km based on the MERIT DEM, https://doi.org/10.5281/zenodo.1447210, 2018.

Hijmans, R. J., Barbosa, M., Bivand, R., Brown, A., Chirico, M., Cordano, E., Dyba, K., Pebesma, E., Rowlingson, B., and Sumner, M. D.: terra: Spatial Data Analysis, 2026.

Höge, M., Kauzlaric, M., Siber, R., Schönenberger, U., Horton, P., Schwanbeck, J., Floriancic, M. G., Viviroli, D., Wilhelm, S., Sikorska-Senoner, A. E., Addor, N., Brunner, M., Pool, S., Zappa, M., and Fenicia, F.: CAMELS-CH: hydro-meteorological time series and landscape attributes for 331 catchments in hydrologic Switzerland, Earth System Science Data, 15, 5755–5784, https://doi.org/10.5194/essd-15-5755-2023, 2023.

Hurrell, J. W., Holland, M. M., Gent, P. R., Ghan, S., Kay, J. E., Kushner, P. J., Lamarque, J.-F., Large, W. G., Lawrence, D., Lindsay, K., Lipscomb, W. H., Long, M. C., Mahowald, N., Marsh, D. R., Neale, R. B., Rasch, P., Vavrus, S.,

https://doi.org/10.5194/essd-2026-350
Preprint. Discussion started: 11 June 2026

Vertenstein, M., Bader, D., Collins, W. D., Hack, J. J., Kiehl, J., and Marshall, S.: The Community Earth System Model: A Framework for Collaborative Research, https://doi.org/10.1175/BAMS-D-12-00121.1, 2013.

James, R., Washington, R., Schleussner, C.-F., Rogelj, J., and Conway, D.: Characterizing half-a-degree difference: a review of methods for identifying regional climate responses to global warming targets, WIREs Climate Change, 8, e457, https://doi.org/10.1002/wcc.457, 2017.

Jimenez, D. A., Meneses, J. E., Solha, P. H. B., Avila-Diaz, A., Quesada, B., Melo Brentan, B., and Ferreira Rodrigues, A.: CAMELS-COL: A Large-Sample Hydrometeorological Dataset for Colombia, Earth System Science Data Discussions, 1–38, https://doi.org/10.5194/essd-2025-200, 2025.

Klingler, C., Schulz, K., and Herrnegger, M.: LamaH-CE: LArge-SaMple DAta for Hydrology and Environmental Sciences for Central Europe, Earth System Science Data, 13, 4529–4565, https://doi.org/10.5194/essd-13-4529-2021, 2021.

Knoben, W. J. M., Thébault, C., Keshavarz, K., Torres-Rojas, L., Chaney, N. W., Pietroniro, A., and Clark, M. P.: Catchment Attributes and MEteorology for Large-Sample SPATially distributed analysis (CAMELS-SPAT): streamflow observations, forcing data and geospatial data for hydrologic studies across North America, Hydrology and Earth System Sciences, 29, 5791–5833, https://doi.org/10.5194/hess-29-5791-2025, 2025.

Koch, J., Liu, J., Stisen, S., Troldborg, L., Højberg, A. L., Thodsen, H., Hansen, M. F. T., and Schneider, R. J. M.: CAMELS-DK: Hydrometeorological Time Series and Landscape Attributes for 3330 Catchments in Denmark (6), https://doi.org/10.22008/FK2/AZXSYP, 2025.

Kraft, B., Schirmer, M., Aeberhard, W. H., Zappa, M., Seneviratne, S. I., and Gudmundsson, L.: CH-RUN: a deep-learning-based spatially contiguous runoff reconstruction for Switzerland, Hydrology and Earth System Sciences, 29, 1061–1082, https://doi.org/10.5194/hess-29-1061-2025, 2025.

Kratzert, F., Klotz, D., Shalev, G., Klambauer, G., Hochreiter, S., and Nearing, G.: Towards learning universal, regional, and local hydrological behaviors via machine learning applied to large-sample datasets, Hydrology and Earth System Sciences, 23, 5089–5110, https://doi.org/10.5194/hess-23-5089-2019, 2019.

Kratzert, F., Nearing, G., Addor, N., Erickson, T., Gauch, M., Gilon, O., Gudmundsson, L., Hassidim, A., Klotz, D., Nevo, S., Shalev, G., and Matias, Y.: Caravan - A global community dataset for large-sample hydrology, Sci Data, 10, 61, https://doi.org/10.1038/s41597-023-01975-w, 2023.

Laake, P. V.: CFtime: Using CF-Compliant Calendars with Climate Projection Data, 2025.

Lee, W.-L., Wang, Y.-C., Shiu, C.-J., Tsai, I. -chun, Tu, C.-Y., Lan, Y.-Y., Chen, J.-P., Pan, H.-L., and Hsu, H.-H.: Taiwan Earth System Model Version 1: description and evaluation of mean state, Geoscientific Model Development, 13, 3887–3904, https://doi.org/10.5194/gmd-13-3887-2020, 2020.

Lees, T., Buechel, M., Anderson, B., Slater, L., Reece, S., Coxon, G., and Dadson, S. J.: Benchmarking data-driven rainfall–runoff models in Great Britain: a comparison of long short-term memory (LSTM)-based models with four lumped conceptual models, Hydrology and Earth System Sciences, 25, 5517–5534, https://doi.org/10.5194/hess-25-5517-2021, 2021.

Loritz, R., Dolich, A., Acuña Espinoza, E., Ebeling, P., Guse, B., Götte, J., Hassler, S. K., Hauffe, C., Heidbüchel, I., Kiesel, J., Mälicke, M., Müller-Thomy, H., Stölzle, M., and Tarasova, L.: CAMELS-DE: hydro-meteorological time series and attributes for 1582 catchments in Germany, Earth System Science Data, 16, 5625–5642, https://doi.org/10.5194/essd-16-5625-2024, 2024.

https://doi.org/10.5194/essd-2026-350
Preprint. Discussion started: 11 June 2026

Mahony, C. R., Wang, T., Hamann, A., and Cannon, A. J.: A global climate model ensemble for downscaled monthly climate normals over North America, Intl Journal of Climatology, 42, 5871–5891, https://doi.org/10.1002/joc.7566, 2022.

Mangukiya, N. K., Kumar, K. B., Dey, P., Sharma, S., Bejagam, V., Mujumdar, P. P., and Sharma, A.: CAMELS-IND: hydrometeorological time series and catchment attributes for 228 catchments in Peninsular India, Earth System Science Data, 17, 461–491, https://doi.org/10.5194/essd-17-461-2025, 2025.

Martel, J.-L., Brissette, F., Arsenault, R., Turcotte, R., Castañeda-Gonzalez, M., Armstrong, W., Mailhot, E., Pelletier-Dumont, J., Rondeau-Genesse, G., and Caron, L.-P.: Assessing the adequacy of traditional hydrological models for climate change impact studies: a case for long short-term memory (LSTM) neural networks, Hydrology and Earth System Sciences, 29, 2811–2836, https://doi.org/10.5194/hess-29-2811-2025, 2025.

Mauritsen, T., Bader, J., Becker, T., Behrens, J., Bittner, M., Brokopf, R., Brovkin, V., Claussen, M., Crueger, T., Esch, M., Fast, I., Fiedler, S., Fläschner, D., Gayler, V., Giorgetta, M., Goll, D. S., Haak, H., Hagemann, S., Hedemann, C., Hohenegger, C., Ilyina, T., Jahns, T., Jimenéz-de-la-Cuesta, D., Jungclaus, J., Kleinen, T., Kloster, S., Kracher, D., Kinne, S., Kleberg, D., Lasslop, G., Kornblueh, L., Marotzke, J., Matei, D., Meraner, K., Mikolajewicz, U., Modali, K., Möbis, B., Müller, W. A., Nabel, J. E. M. S., Nam, C. C. W., Notz, D., Nyawira, S.-S., Paulsen, H., Peters, K., Pincus, R., Pohlmann, H., Pongratz, J., Popp, M., Raddatz, T. J., Rast, S., Redler, R., Reick, C. H., Rohrschneider, T., Schemann, V., Schmidt, H., Schnur, R., Schulzweida, U., Six, K. D., Stein, L., Stemmler, I., Stevens, B., von Storch, J.-S., Tian, F., Voigt, A., Vrese, P., Wieners, K.-H., Wilkenskjeld, S., Winkler, A., and Roeckner, E.: Developments in the MPI-M Earth System Model version 1.2 (MPI-ESM1.2) and Its Response to Increasing CO2, Journal of Advances in Modeling Earth Systems, 11, 998–1038, https://doi.org/10.1029/2018MS001400, 2019.

Miralles, D. G., Holmes, T. R. H., De Jeu, R. a. M., Gash, J. H., Meesters, A. G. C. A., and Dolman, A. J.: Global land-surface evaporation estimated from satellite-based observations, Hydrology and Earth System Sciences, 15, 453–469, https://doi.org/10.5194/hess-15-453-2011, 2011.

Morin, E.: Caravan extension Israel - Israel dataset for large-sample hydrology, https://doi.org/10.5281/zenodo.15003600, 2025.

Morton, F. I.: Operational estimates of areal evapotranspiration and their significance to the science and practice of hydrology, Journal of Hydrology, 66, 1–76, https://doi.org/10.1016/0022-1694(83)90177-4, 1983.

Muñoz Sabater, J.: ERA5-Land monthly averaged data from 1950 to present, https://doi.org/10.24381/cds.68d2bb30, 2019.

do Nascimento, T. V. M., Höge, M., Schönenberger, U., Pool, S., Siber, R., Kauzlaric, M., Staudinger, M., Horton, P., Floriancic, M. G., Storck, F. R., Rinta, P., Seibert, J., and Fenicia, F.: Swiss data quality: augmenting CAMELS-CH with isotopes, water quality, agricultural and atmospheric data, Sci Data, 12, 1283, https://doi.org/10.1038/s41597-025-05625-1, 2025.

National Oceanic and Atmospheric Administration, National Aeronautics and Space Administration, and United States Air Force: U.S. Standard Atmosphere, 1976, 1976.

nc-time-axis contributors: nc-time-axis: Provides support for a cftime axis in matplotlib, 2026.

Newman, A. J., Clark, M. P., Sampson, K., Wood, A., Hay, L. E., Bock, A., Viger, R. J., Blodgett, D., Brekke, L., Arnold, J. R., Hopson, T., and Duan, Q.: Development of a large-sample watershed-scale hydrometeorological data set for the contiguous USA: data set characteristics and assessment of regional variability in hydrologic model performance, Hydrology and Earth System Sciences, 19, 209–223, https://doi.org/10.5194/hess-19-209-2015, 2015.

https://doi.org/10.5194/essd-2026-350
Preprint. Discussion started: 11 June 2026

Priestley, C. H. B. and Taylor, R. J.: On the Assessment of Surface Heat Flux and Evaporation Using Large-Scale Parameters, Mon. Wea. Rev., 100, 81–92, https://doi.org/10.1175/1520-0493(1972)100%3C0081:OTAOSH%3E2.3.CO;2, 1972.

Rahimpour Asenjan, M., Brissette, F., Martel, J.-L., and Arsenault, R.: Understanding the influence of "hot" models in climate impact studies: a hydrological perspective, Hydrology and Earth System Sciences, 27, 4355–4367, https://doi.org/10.5194/hess-27-4355-2023, 2023.

Ruzzante, S.: Caravan-CMIP6: Bias-corrected climate model projections for ten large-sample hydrometeorological datasets and over 23,000 global catchments, https://doi.org/10.20383/103.01644, 2026.

Ruzzante, S. W., Knoben, W. J. M., Wagener, T., Gleeson, T., and Schnorbus, M.: Technical note: High Nash–Sutcliffe Efficiencies conceal poor simulations of interannual variance in seasonal regimes, Hydrology and Earth System Sciences, 30, 2337–2355, https://doi.org/10.5194/hess-30-2337-2026, 2026.

Sellar, A. A., Jones, C. G., Mulcahy, J. P., Tang, Y., Yool, A., Wiltshire, A., O'Connor, F. M., Stringer, M., Hill, R., Palmieri, J., Woodward, S., de Mora, L., Kuhlbrodt, T., Rumbold, S. T., Kelley, D. I., Ellis, R., Johnson, C. E., Walton, J., Abraham, N. L., Andrews, M. B., Andrews, T., Archibald, A. T., Berthou, S., Burke, E., Blockley, E., Carslaw, K., Dalvi, M., Edwards, J., Folberth, G. A., Gedney, N., Griffiths, P. T., Harper, A. B., Hendry, M. A., Hewitt, A. J., Johnson, B., Jones, A., Jones, C. D., Keeble, J., Liddicoat, S., Morgenstern, O., Parker, R. J., Predoi, V., Robertson, E., Siahaan, A., Smith, R. S., Swaminathan, R., Woodhouse, M. T., Zeng, G., and Zerroukat, M.: UKESM1: Description and Evaluation of the U.K. Earth System Model, Journal of Advances in Modeling Earth Systems, 11, 4513–4558, https://doi.org/10.1029/2019MS001739, 2019.

Shalev, G. and Kratzert, F.: Caravan MultiMet: Extending Caravan with Multiple Weather Nowcasts and Forecasts, https://doi.org/10.48550/arXiv.2411.09459, 14 November 2024.

Shen, H., Tolson, B. A., and Mai, J.: Time to Update the Split-Sample Approach in Hydrological Model Calibration, Water Resources Research, 58, e2021WR031523, https://doi.org/10.1029/2021WR031523, 2022.

Sherwood, S. C., Webb, M. J., Annan, J. D., Armour, K. C., Forster, P. M., Hargreaves, J. C., Hegerl, G., Klein, S. A., Marvel, K. D., Rohling, E. J., Watanabe, M., Andrews, T., Braconnot, P., Bretherton, C. S., Foster, G. L., Hausfather, Z., von der Heydt, A. S., Knutti, R., Mauritsen, T., Norris, J. R., Proistosescu, C., Rugenstein, M., Schmidt, G. A., Tokarska, K. B., and Zelinka, M. D.: An Assessment of Earth's Climate Sensitivity Using Multiple Lines of Evidence, Reviews of Geophysics, 58, e2019RG000678, https://doi.org/10.1029/2019RG000678, 2020.

Singer, M. B., Asfaw, D. T., Rosolem, R., Cuthbert, M. O., Miralles, D. G., MacLeod, D., Quichimbo, E. A., and Michaelides, K.: Hourly potential evapotranspiration at 0.1° resolution for the global land surface from 1981-present, Sci Data, 8, 224, https://doi.org/10.1038/s41597-021-01003-9, 2021.

Swart, N. C., Cole, J. N. S., Kharin, V. V., Lazare, M., Scinocca, J. F., Gillett, N. P., Anstey, J., Arora, V., Christian, J. R., Hanna, S., Jiao, Y., Lee, W. G., Majaess, F., Saenko, O. A., Seiler, C., Seinen, C., Shao, A., Sigmond, M., Solheim, L., von Salzen, K., Yang, D., and Winter, B.: The Canadian Earth System Model version 5 (CanESM5.0.3), Geoscientific Model Development, 12, 4823–4873, https://doi.org/10.5194/gmd-12-4823-2019, 2019.

Tatebe, H., Ogura, T., Nitta, T., Komuro, Y., Ogochi, K., Takemura, T., Sudo, K., Sekiguchi, M., Abe, M., Saito, F., Chikira, M., Watanabe, S., Mori, M., Hirota, N., Kawatani, Y., Mochizuki, T., Yoshimura, K., Takata, K., O'ishi, R., Yamazaki, D., Suzuki, T., Kurogi, M., Kataoka, T., Watanabe, M., and Kimoto, M.: Description and basic evaluation of simulated mean state, internal variability, and climate sensitivity in MIROC6, Geoscientific Model Development, 12, 2727–2765, https://doi.org/10.5194/gmd-12-2727-2019, 2019.

https://doi.org/10.5194/essd-2026-350
Preprint. Discussion started: 11 June 2026

Thrasher, B., Maurer, E. P., McKellar, C., and Duffy, P. B.: Technical Note: Bias correcting climate model simulated daily temperature extremes with quantile mapping, Hydrology and Earth System Sciences, 16, 3309–3314, https://doi.org/10.5194/hess-16-3309-2012, 2012.

Tran, V. N., Xu, D., Van Nguyen, T., Kim, T., and Ivanov, V. Y.: CAMELSH: A Large-Sample Hourly Hydrometeorological Dataset and Attributes at Watershed-Scale for CONUS, Sci Data, 12, 1307, https://doi.org/10.1038/s41597-025-05612-6, 2025.

University of Waterloo: Canada's most powerful academic supercomputer launched at University of Waterloo, , 15th May, 2017.

Vicente-Serrano, S. M., Beguería, S., and López-Moreno, J. I.: A Multiscalar Drought Index Sensitive to Global Warming: The Standardized Precipitation Evapotranspiration Index, https://doi.org/10.1175/2009JCLI2909.1, 2010.

Voldoire, A., Saint-Martin, D., Sénési, S., Decharme, B., Alias, A., Chevallier, M., Colin, J., Guérémy, J.-F., Michou, M., Moine, M.-P., Nabat, P., Roehrig, R., Salas y Mélia, D., Séférian, R., Valcke, S., Beau, I., Belamari, S., Berthet, S., Cassou, C., Cattiaux, J., Deshayes, J., Douville, H., Ethé, C., Franchistéguy, L., Geoffroy, O., Lévy, C., Madec, G., Meurdesoif, Y., Msadek, R., Ribes, A., Sanchez-Gomez, E., Terray, L., and Waldman, R.: Evaluation of CMIP6 DECK Experiments With CNRM-CM6-1, Journal of Advances in Modeling Earth Systems, 11, 2177–2213, https://doi.org/10.1029/2019MS001683, 2019.

Volodin, E. and Gritsun, A.: Simulation of observed climate changes in 1850–2014 with climate model INM-CM5, Earth System Dynamics, 9, 1235–1242, https://doi.org/10.5194/esd-9-1235-2018, 2018.

Whitaker, J., Clark, S., Khrulev, C., Filipe, Hoese, D., Little, B., May, R., Hassell, D., Larson, E., Lindsley, R., McGibbon, J., Cuntz, M., Huard, D., Robert, C., Henderson, B. H., Hoyer, S., Heerdegen, A., Banihirwe, A., Clauss, C., Penn, J., Bruick, Z., Decker, M., Pagani, B., Gohlke, C., Rusak, J., Magin, J., Brett, M., Hetland, R., and Stefan: Unidata/cftime: version 1.6.5 release, , https://doi.org/10.5281/zenodo.17342944, 2025.

Wu, G., Chen, J., Shi, X., Kim, J.-S., Xia, J., and Zhang, L.: Impacts of Global Climate Warming on Meteorological and Hydrological Droughts and Their Propagations, Earth's Future, 10, e2021EF002542, https://doi.org/10.1029/2021EF002542, 2022.

Yamazaki, D., Ikeshima, D., Tawatari, R., Yamaguchi, T., O'Loughlin, F., Neal, J. C., Sampson, C. C., Kanae, S., and Bates, P. D.: A high-accuracy map of global terrain elevations, Geophysical Research Letters, 44, 5844–5853, https://doi.org/10.1002/2017GL072874, 2017.

Yukimoto, S., Kawai, H., Koshiro, T., Oshima, N., Yoshida, K., Urakawa, S., Tsujino, H., Deushi, M., Tanaka, T., Hosaka, M., Yabu, S., Yoshimura, H., Shindo, E., Mizuta, R., Obata, A., Adachi, Y., and Ishii, M.: The Meteorological Research Institute Earth System Model Version 2.0, MRI-ESM2.0: Description and Basic Evaluation of the Physical Component, Journal of the Meteorological Society of Japan. Ser. II, 97, 931–965, https://doi.org/10.2151/jmsj.2019-051, 2019.

Zajaczkowski, J. and Jeffrey, S.: Potential evaporation and evapotranspiration data provided by SILO, Department of Environment and Science, Queensland Government, 2020.

Ziehn, T., Chamberlain, M. A., Law, R. M., Lenton, A., Bodman, R. W., Dix, M., Stevens, L., Wang, Y.-P., and Srbinovsky, J.: The Australian Earth System Model: ACCESS-ESM1.5, JSHESS, 70, 193–214, https://doi.org/10.1071/ES19035, 2020.